BCL-2 Modifying Factor (BMF) Is a Central Regulator of Anoikis in Human Intestinal Epithelial Cells*[S]

Martin Hausmann[‡1], Katharina Leucht[‡], Christian Ploner[§2], Stephan Kiessling[¶], Andreas Villunger[¶], Helen Becker[¶], Claudia Hofmann[‖], Werner Falk[‖], Michaela Krebs[‡], Silvia Kellermeier[‡], Michael Fried[‡], Jürgen Schölmerich[‖], Florian Obermeier[‖3], and Gerhard Rogler[‡]

From the [‡]Division of Gastroenterology and Hepatology, Department of Internal Medicine, University Hospital of Zürich, 8091 Zürich, Switzerland, the [§]Division of Molecular Pathophysiology and [¶]Division of Developmental Immunology, Biocenter, Medical University Innsbruck, 6020 Innsbruck, Austria, and the [‖]Department of Internal Medicine I, University of Regensburg, 93053 Regensburg, Germany

BCL-2 modifying factor (BMF) is a sentinel considered to register damage at the cytoskeleton and to convey a death signal to B-cell lymphoma 2. B-cell lymphoma 2 is neutralized by BMF and thereby facilitates cytochrome C release from mitochondria. We investigated the role of BMF for intestinal epithelial cell (IEC) homeostasis. Acute colitis was induced in *Bmf*-deficient mice (*Bmf*⁻/⁻) with dextran sulfate sodium. Colonic crypt length in *Bmf*⁻/⁻ mice was significantly increased as compared with WT mice. Dextran sulfate sodium induced less signs of colitis in *Bmf*⁻/⁻ mice, as weight loss was reduced compared with the WT. Primary human IEC exhibited increased BMF in the extrusion zone. Quantitative PCR showed a significant up-regulation of *BMF* expression after initiation of anoikis in primary human IEC. BMF was found on mitochondria during anoikis, as demonstrated by Western blot analysis. RNAi mediated knockdown of *BMF* reduced the number of apoptotic cells and led to reduced caspase 3 activity. A significant increase in phospho-AKT was determined after RNAi treatment. *BMF* knockdown supports survival of IEC. BMF is induced in human IEC by the loss of cell attachment and is likely to play an important role in the regulation of IEC survival.

Intestinal epithelial cells (IEC)[4] are generated from stem cells at the base of the crypt and migrate on the underlying basement membrane toward the intestinal lumen in 3–5 days. There apoptosis is initiated, and cells finally lose anchorage and are shed into the lumen (1–4). IEC undergo apoptosis when they lose their contact with the extracellular matrix (5), a phenomenon termed "anoikis" (6). This special form of cell death is an important mechanism terminating the physiological life cycle of IEC (7–12). In contrast, carcinoma cells are resistant to anoikis, which is one of the prerequisites for cancer development (13, 14).

The activation of the apoptotic cascade leads to the cleavage of various structurally and functionally essential intracellular substrate proteins (15). We demonstrated recently that the preservation of cell-cell contacts and cell-matrix anchorage maintains both intercellular attachment and crypt structure, diminishing initiation of the apoptotic cascade (16). Members of the B-cell lymphoma (BCL)-2 family of proteins decide over the life or death of a cell. BCL-2 is located on the outer mitochondrial membrane and prevents the release of cytochrome C from the mitochondrion. BCL-2 can interact with BMF (BCL-2-modifying factor), a member of the proapoptotic BH3-only protein subgroup of the BCL-2 family. BMF was first described in 2001 (17) and initially discussed to transduce death signals caused by different forms of cell stress, such as UV irradiation or loss of contact to the extracellular matrix, *i.e.* anoikis, or inhibition of the CAP-dependent translation machinery (18). However, studies in different cell types from *Bmf*-deficient mice suggested redundancy with other BH3-only proteins during most of these cell death processes (19). BMF interacts intracellularly with the dynein light chain 2 (DLC2), a component of the myosin V motor complex. By this, BMF can be separated from BCL-2. Some stress stimuli have been reported to induce the release of BMF from the complex and its translocation to mitochondria (17, 20). Mutations in the light chain-binding domain of BMF enhance the death-promoting activity of this protein in cell culture (17). BMF (as well as BAD, NOXA, and PUMA) is also considered to act as sensitizer that binds prosurvival BCL-2 protein to displace activator BH3-only proteins (*i.e.* BID or BCL-2-interacting mediator of cell death (BIM)) from BCL-2 to promote cell death (21). The interaction of BMF with BCL-2 on the mitochondrial surface neutralizes the anti-apoptotic action of BCL-2. Activator BH3-only proteins bind BAX and BAK, essential for mitochondrial apoptosis by forming pores in the mitochondrial membrane, and induce the release of cytochrome C, finally triggering apoptosis. Alternatively, BMF may contribute to the neutralization of prosurvival pro-

[4] The abbreviations used are: IEC, intestinal epithelial cell(s); BCL, B-cell lymphoma; BMF, B-cell lymphoma-modifying factor; DSS, dextran sulfate sodium; BIM, BCL-2-interacting mediator of cell death.

teins present in a cell, considered equally sufficient to induce apoptosis (22).

BMF transduces death signals not only after release from the actin cytoskeleton but also by activation of transcription. *BMF* transcription is induced by TGFβ-driven apoptosis in a number of cell types (23). TGFβ-induced autophagy potentiates the induction of the proapoptotic proteins BMF and BIM by the stress-responsive transcription factor CHOP upon growth factor withdrawal (24). Once BCL-2 is neutralized and cytochrome C is released out of the mitochondrion, the so-called "apoptosome" is built, inducing a proteolytic cascade of caspases (25–29). During anoikis of human IEC, caspases 2 and 9 are reportedly involved in the initiation of anoikis and activate downstream effector caspases 7, 3, and 6 (30). This results in a sequential cleavage of focal adhesion kinase by caspase 3 and caspase 6 (31) and culminates in characteristic apoptotic morphological changes.

Together, this suggests that BMF may be critical for epithelial cell homeostasis. We investigated the role of BMF for cell death of IEC in mice under inflammatory conditions as well as in isolated primary human IEC.

EXPERIMENTAL PROCEDURES

Patients—Primary human IEC were obtained from surgical specimens from intestinal mucosa of 62 patients undergoing surgery in the large or small bowel ($>$ 10 cm of distance from the tumor for carcinoma patients, supplemental Table 1). 34 patients were male, and 28 patients were female. The patients were between 17 and 89 (mean 51 $\pm$ 17) years of age. This study was approved by the Ethics Committees of the University of Regensburg and the University of Zürich and performed according to the Declaration of Helsinki.

Induction and Treatment of DSS Colitis—Male C57BL/6-*Bmf*^tm1.1Anvi (*Bmf*$^{-/-}$) mice were backcrossed for at least 12 generations (19). Mice weighing 25–32 g were used for the experiments and housed in individually ventilated cages. Acute colitis was induced as described previously (32). During induction of acute colitis, mice received either 3.5% DSS in drinking water or drinking water alone over 8 days. Animals were provided unlimited access to food and water throughout the experiment (*ad libitum*). Mice were killed on day 8. From the distal third of the colon, 1 cm of colonic tissue was removed and used for histological analysis, as described previously (32, 33).

Cell Lines, IEC Isolation, and Induction of Anoikis—Cells were grown in RPMI 1640 (Bio-Whitaker, Verviers, Belgium) supplemented with 10% FCS, 100 units/ml penicillin, 100 μg/ml streptomycin, and 2 mM L-glutamine (Gibco, Invitrogen cell culture) at 37 °C, 5% CO_2. HEK293T packaging cells for lentivirus production were grown in DMEM (Bio-Whitaker) containing 10% FCS, 100 units/ml penicillin, 100 μg/ml streptomycin, and 2 mM L-glutamine (Gibco).

IEC were isolated as described in Ref. 34 and in the supplemental material. For induction of anoikis, IEC were liberated from crypts by agitation at 37 °C on a whip-shaker.

Antibodies—Primary antibodies used were rat anti-BMF IgG2a (#9G10, Alexis, Lörrach, Germany, 1:500), rabbit anti-human BMF (#ab59906, Abcam, Cambridge, UK, 1:100), rabbit anti-cleaved caspase 3 (Asp175, #9661, Cell Signaling Technol-

ogy, Inc., Beverly, MA, 1:3000), mouse anti-caspase 3 IgG2a (#610322, BD Biosciences, 1:3000), rabbit anti-phospho-AKT (#9271, Cell Signaling Technology, Inc., 1:1000), mouse anti-caspase 6 IgG1 (#556581, BD Biosciences, 1:1000), rabbit anti-cleaved caspase 6 (#9761, Cell Signaling Technology, Inc., 1:1000), mouse anti-caspase 7 IgG1 (#9494, Cell Signaling Technology, Inc., 1:1000), mouse anti-human cytochrome C oxidase, mitochondria complex (COX) IV (#MS408, Acris, 1:2000), and mouse anti-β-actin IgG1 (#sc8432, Santa Cruz Biotechnology, Inc., 1:10 000).

Isotype controls used were rat IgG2a (#ab18450, Abcam) and rabbit and mouse IgG (sc-2027 and sc-2025, Santa Cruz Biotechnology, Inc.). Secondary antibodies used were Alexa Fluor 488 goat anti-rat IgG (#A11006, Molecular Probes, Inc., OR, 1:300), goat anti-rat IgG, goat anti-rabbit IgG, and goat-anti-mouse IgG (IgG-HRP, sc-2006, sc-2004, sc-2005, Santa Cruz Biotechnology, Inc., 1:5000).

Digitonin-based Subcellular Fractionation and Western Blot Analysis—For isolation of mitochondria, IEC (3×10^7) were washed in ice-cold PBS. Cells were digitonin-permeabilized in 1 ml of cytosolic extraction buffer (200 μg/ml digitonin (#D141, Sigma) and a complete mini tablet (#04 693 124 001, Roche) in 250 mM sucrose, 70 mM KCl, 137 mM NaCl, 4.3 mM Na_2HPO_4, 1.4 mM KH_2PO_4 (pH 7.2)). Plasma membrane permeabilization of cells was confirmed by staining in a trypan blue solution. Cells were centrifuged at 1000 $\times$ *g* for 5 min at 4 °C. The supernatant (cytosolic fraction) was saved, and the pellets were solubilized in the same volume of mitochondrial lysis buffer (50 mM Tris, 150 mM NaCl, 2 mM EDTA, 2 mM EGTA, 0.2% Triton X-100, 0.3% Nonidet P-40, and a complete mini tablet (pH 7.4)), followed by pelleting at 10,000 $\times$ *g* for 10 min at 4 °C. The supernatant was collected as mitochondrial fraction. Western blot analysis was performed as described in the supplemental material and in Ref. 16.

Virus Generation and Transfection—Vector cloning and infections were performed as described in the supplemental material and in Ref. 35. Human mucosa for viral transduction was transferred immediately after surgery in the viral supernatant. Isolation of intestinal crypts was performed in lentivirus-containing media. Isolation was finished within a time period of 1.5 h. Crypts were then kept on collagen-coated transwells at 37 °C and 5% CO_2 in lentivirus-containing media. After 24 h on transwells, IEC were isolated. Including the transport time of the resection from the department of surgery, IEC were kept in virus-containing media for 25.5 h. After 25.5 h, IEC were isolated.

Statistical Analysis—Real-time PCR data were calculated from triplicates. Statistical analysis was performed using the Mann-Whitney rank sum test. One-way analysis of variance was used for body weight, colon length, and real-time PCR if four groups were compared. The Mann-Whitney rank sum test was used for crypt length, real-time PCR if two groups were compared, Western blot analysis. Data are expressed as mean $\pm$ S.D. Differences were considered significant at $p < 0.05$ (*), highly significant at $p < 0.01$ (**), and very highly significant at $p < 0.001$ (***). For statistical analysis of Western blot analyses, luminescence signals were determined by densitometry and
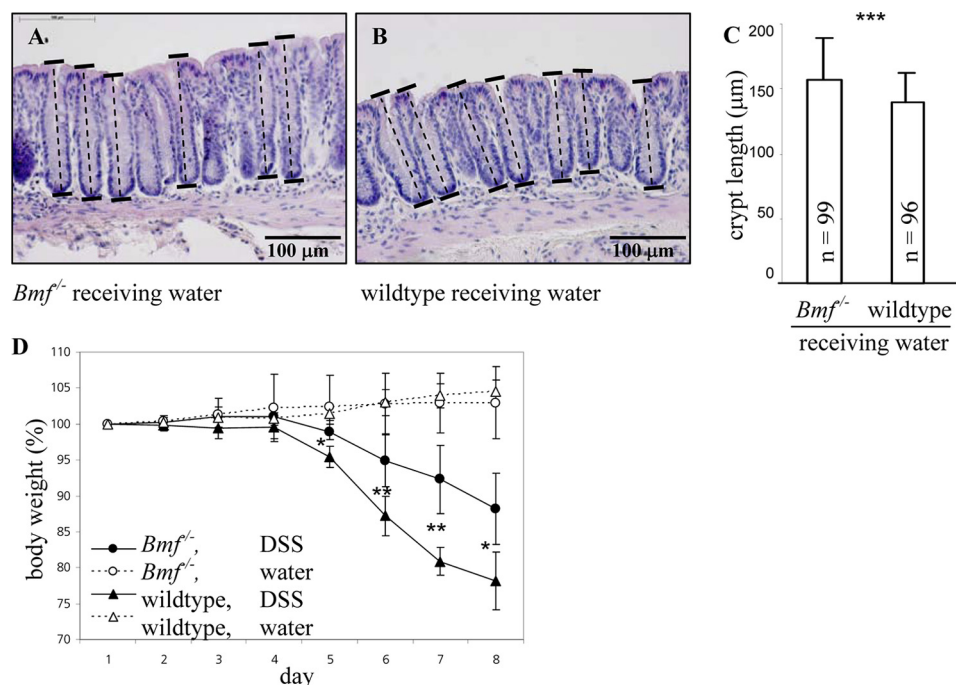
FIGURE 1. **Crypt length and body weight loss.** Crypt lengths for $Bmf^{-/-}$ mice receiving water (*A*) and wild-type mice receiving water (*B*). A section 0–1 cm from the distal end of the colon is shown. *C*, a normality test for crypt length in $Bmf^{-/-}$ mice and wild-type mice receiving water failed, and a Mann-Whitney rank sum test was performed. $Bmf^{-/-}$ mice showed a significantly increased crypt length compared with wild-type mice. ***, $p < 0.001$. *D*, $Bmf^{-/-}$ mice (○ and ●) and wild-type mice (△ and ▲) received either DSS (▲) or water (△). *Bars* represent mean ± S.D. One-way analysis of variance was used. Body weight loss was significantly different for wild-type mice upon DSS treatment compared with $Bmf^{-/-}$ mice upon DSS treatment on days 5, 6, 7, and 8. Day 5, $p = 0.016$; day 6, $p = 0.008$; day 7, $p = 0.007$; and day 8, $p = 0.016$; $n = 5$ each. $Bmf^{-/-}$ mice showed a significantly decreased body weight loss upon DSS treatment and increased crypt length upon water treatment.

quantified with the OptiQuant software (Packard Instrument Co., Meriden, CT).

RESULTS

Crypt Structures Are Protected in $Bmf^{-/-}$ Mice upon DSS Colitis—We focused on the involvement of BMF in inflammatory responses and its property to induce apoptosis in IEC. Colonic crypt lengths for $Bmf^{-/-}$ mice were significantly increased compared with the wild type (156.9 ± 32.0 μm, $n = 99$ and 139.8 ± 22.4 μm, $n = 96$, calculated from sections of five mice, respectively, $p < 0.05$, Fig. 1, *A–C*). A hydrometrocolpos was described in female $Bmf^{-/-}$ mice. Confirmative to this, we observed an enlarged uterovaginal tract in $Bmf^{-/-}$ mice.

We used the DSS colitis mouse model to determine BMF dependence of mucosal inflammation. During induction of acute colitis, mice received 3.5% DSS in drinking water ($n = 10$) or drinking water alone ($n = 10$) over 8 days. Water consumption was not reduced in mice treated with DSS (126 ml for $Bmf^{-/-}$ mice with DSS, 121 ml for $Bmf^{-/-}$ mice with water, 119 ml for wild-type mice with DSS, and 122 ml for wild-type mice with water, $n = 5$ each). Upon DSS administration, weight loss of $Bmf^{-/-}$ mice was significantly decreased from days 5–8 compared with wild-type mice (Fig. 1*D*). Upon DSS administration, no blood was visible on the anus of $Bmf^{-/-}$ mice, whereas two wild-type mice displayed blood on the anus from days 4–8, and four wild-type mice displayed blood on the anus from days 5–8. Upon DSS administration, no aggressive behavior was observed in cages with $Bmf^{-/-}$ mice, whereas wild-type mice showed aggressive behavior from days 4–8. Induction of colitis was followed by a typical and significant reduction of

colon length (supplemental Fig. 1, *A and B*). $Bmf^{-/-}$ mice with and without colitis showed an increased colon length.

Previous experimental evidence reported impaired cell death in lymphocytes in the absence of BMF, but no significant differences between wild-type and $Bmf^{-/-}$ mice IEC undergoing cell death *in vitro* were noted (19). Consistently, we failed to observe differences in the histological score between $Bmf^{-/-}$ and wild-type mice receiving water (0.9 ± 0.4 for $Bmf^{-/-}$ mice and 1.3 ± 0.8 for wild-type mice, $n = 5$ each). The histological score for $Bmf^{-/-}$ mice and wild-type mice receiving DSS was also not altered significantly (7.6 ± 0.4 and 7.4 ± 0.7, respectively).

To locate apoptotic cells in colonic tissue, we performed a TUNEL analysis. Cleavage of genomic DNA during apoptosis was found in an expected dimension. Apoptosis was not uniform along the crypt-villus axis. In crypts, positively stained cells were preferentially detected apically, close to the lumen. Confirmative to previous findings based on FACS analysis, TUNEL staining revealed no decrease in apoptosis from colonic IEC lacking BMF *in situ* (supplemental Fig. 1, *C–F*). Mucosa from mice suffering from DSS colitis showed extensive epithelial damage and both infiltration and thickening of the mucosa. In wild-type and $Bmf^{-/-}$ mice receiving DSS, crypt morphology was absent, and goblet cells were lost. To detect remaining IEC, epithelial cell adhesion molecule (EpCAM) staining was performed. 45 ± 37% of IEC remained as a layer on the thickened mucosa of the distal end of the colon in $Bmf^{-/-}$ mice upon DSS treatment compared with 34 ± 33% in DSS-treated wild-type mice (supplemental Fig. 1, *G and H*).
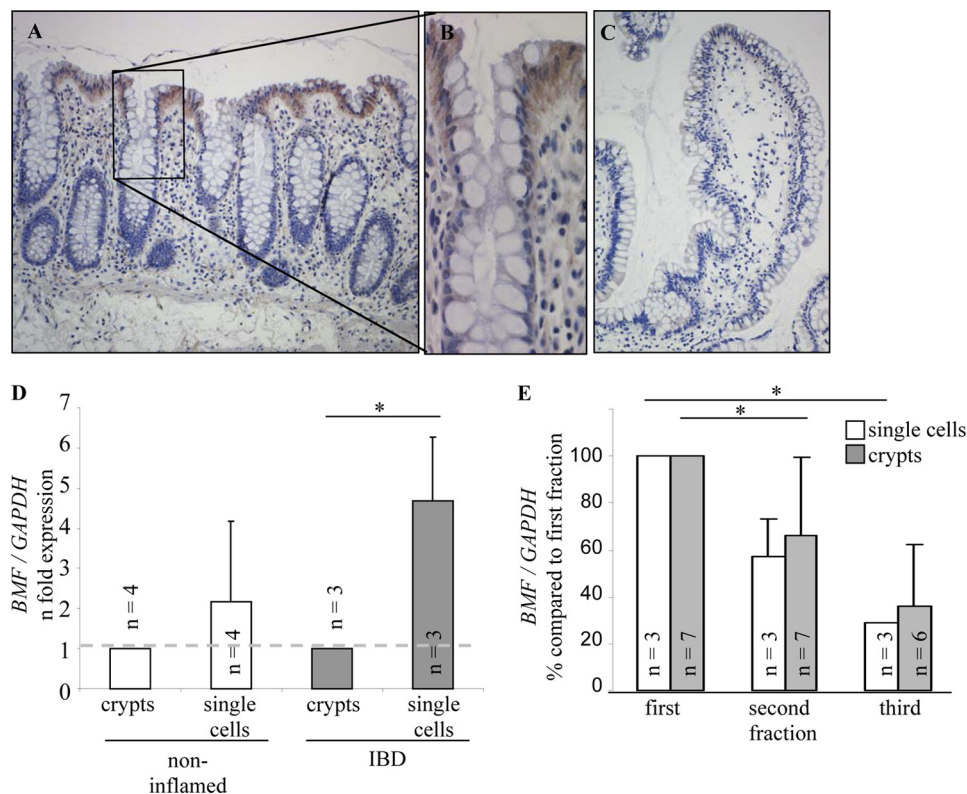
FIGURE 2. **Immunohistochemistry for BMF on sections from human (*A* and *B*) large intestine and (*C*) small intestine.** *A* and *B*, immunostaining of BMF on section from a Crohn's disease patient without inflammation. *C*, negative control without primary antibody. Immunohistochemistry revealed an expression gradient of BMF along the crypt-villus axis. The 3′, 3′-diaminobenzidine (DAB) procedure was used. Original magnification (*A* and *C*) × 100, and × 200 (*B*). *D*, *BMF* is significantly increased in single IEC from inflammatory bowel disease patients compared with crypts. *E*, *BMF* is down-regulated in IEC isolated in subsequent agitation procedures in both single cells and crypts. IEC were isolated by three successive agitation procedures, and *BMF* expression was analyzed by real-time PCR. One-way analysis of variance was used. *, $p < 0.05$.

BMF Expression Is Induced along the Human Crypt-Villus Axis—IEC mature along the crypt-villus axis. Maturation is reflected in both changes of gene expression and transition from an epithelial stem cell, firmly embedded in the crypt, to a cell intrinsically prone to anoikis and prepared to be detached. BMF on mitochondria results in cytochrome C release from mitochondria and activation of the caspase cascade, leading to apoptosis. Immunohistochemistry was performed to localize BMF in human colonic sections. IEC exhibited intense staining in the extrusion zone where cells are expected to be shed. Brown staining was found in IEC in human mucosa (Fig. 2, *A* and *B*). IEC were isolated from patients by three successive agitation procedures. Single cells were separated from whole crypts, and the relative amount of *BMF* cDNA was calculated by means of real-time PCR. Data from crypts were set to 1. *BMF* mRNA in single IEC from patients without inflammatory bowel disease was 2.2 ± 2-fold increased compared with crypts (Fig. 2*D*). *BMF* mRNA in single cells from patients with inflammatory bowel disease was increased significantly (4.8 ± 1.5-fold, Mann-Whitney rank sum test, $p < 0.05$) compared with crypts. The same trend was found for *PUMA* and *BID* without reaching statistical significance (supplemental Fig. 2, *A* and *B*). Human IEC were fractionated during the isolation procedure according to their capacity of staying attached to the colonic mucosa. *BMF* mRNA was down-regulated in IEC obtained in second and third fractions (Fig. 2*E*). Data from the first IEC fraction of each surgical specimen were set to 100%. Significant differences

were determined between the first and the second crypt fraction ($-66 \pm 32\%$) and the first and the third fraction of single cells ($-29 \pm 3\%$, analysis of variance multiple variance analysis, $p < 0.05$).

BMF Is Up-regulated and Found on Mitochondria during Anoikis—Anoikis is the inevitable end of the IEC life cycle. Anoikis is also inducible by disconnecting cell-cell and cell-matrix contacts, as described under "Experimental Procedures." Real-time PCR was performed from freshly isolated human IEC and detached IEC 2 h after *ex vivo* isolation from 19 surgical specimens. The initiation of anoikis is followed by a significant up-regulation of *BMF* mRNA ($p < 0.05$, Fig. 3*A*). Significant up-regulation was found for *PUMA* (supplemental Fig. 3, Mann-Whitney rank sum test, $p < 0.05$).

We examined the BMF level in mitochondria from human IEC after the induction of anoikis. Cells from the last of the three successive agitation procedures were used. Mitochondria were prepared from freshly isolated IEC and from IEC incubated without matrix contact for 2 h after *ex vivo* isolation. Fig. 3*B* shows BMF in the mitochondrial fraction 2 h after induction of anoikis (23 and 25 kDa, *upper panel*). This could be due to higher expression levels. Immediately after isolation of IEC, BMF was barely visible in the mitochondrial fraction.

Knockdown of BMF Reduces Anoikis in Human IEC—Anoikis is initiated following neutralization of the antiapoptotic BCL-2 proteins through association of BMF and/or other BH3-only proteins. HEK293T were transfected for virus assembly. Devel-
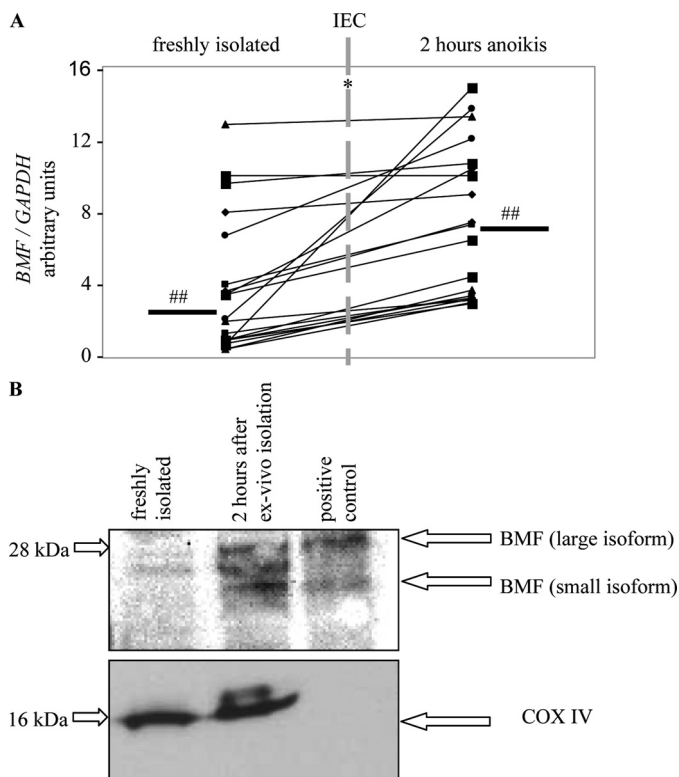
FIGURE 3. **Initiation of anoikis is followed by up-regulation of BMF.** *A*, real-time PCR of freshly isolated human IEC and human IEC 2 h after *ex vivo* isolation. A Mann-Whitney rank sum test was performed. $p < 0.05$. $n = 19$. ##, median. *B*, Western blot analysis of mitochondrial fractions of freshly isolated IEC and IEC 2 h after *ex vivo* isolation. A third BMF isoform seen in human IEC lysates was not detected in extracts from mouse spleen used as positive control. Western blot analysis for COX IV (18 kDa) showed successful purification of mitochondria and demonstrated equal loading in the human IEC samples analyzed but, as expected, was not detected in the mouse extract because of specificity to the human protein (*lower panel*). Loss of cytochrome C (15 kDa) was only marginal 2 h after *ex vivo* isolation (not shown). Data are representative for three patients.

opment of virus in supernatants and efficient transduction was confirmed (supplemental material and Fig. 4, *A–E*). Including the transport of the resection from the department of surgery, isolation of crypts, and incubation on transwells, IEC were kept in virus-containing media for 25.5 h. Efficient infection of human crypts, kept on collagen-coated transwells, was confirmed by fluorescence microscopy (Fig. 4*A*). Viability of IEC was confirmed by trypan blue staining (Fig. 4*B*). Knockdown of *BMF* in IEC was confirmed by determining BMF with Western blot analysis (Fig. 4*C*). Efficient down-regulation of *BMF* mRNA in infected IEC was confirmed by real-time PCR. Mock-infected IEC had a *BMF/GAPDH* ratio of 8.0 ± 5.8 ($n = 3$), and virus-infected cells had a *BMF/GAPDH* ratio of 0.2 ± 0.2 ($n = 3$). We investigated whether knockdown of *BMF* by the lentiviral system was able to delay anoikis in human IEC. For fluorescence microscopy, cells were mounted with medium containing DAPI. Freshly isolated human IEC displayed round nuclei, revealing no indication of anoikis (Fig. 4*D*). To induce anoikis, single IEC were liberated from isolated crypts by agitation at 37 °C on a whip-shaker in media including EDTA for 2 h and harvested by centrifugation. Fluorescence microscopy showed cells with a disintegrated nuclei pattern, a clear sign of ongoing execution of anoikis (Fig. 4*E*). No round nuclei were found. Fig.

4*F* shows cells with *BMF* knockdown 2 h after induction of anoikis. The number of apoptotic nuclei was lower than in the experiments without knockdown, as a number of round nuclei were found. These data show that *BMF* knockdown in human IEC is capable of preserving cellular morphology.

Knockdown of BMF Maintains Phosphorylation of AKT and Blocks Activation of Caspases—Including the transport time of the resection from the department of surgery, isolation of crypts, and incubation on transwells, IEC were kept in virus-containing media for 25.5 h. Phosphorylation of the important prosurvival signaling molecule AKT in human crypts, isolated within the first fraction of IEC, was determined by Western blot analysis. AKT reportedly promotes cell survival by inhibiting anoikis via phosphorylation and inactivation of several proapoptotic targets, including BAD and caspase 9 (16). Phosphorylation, and thereby activation, of the protein kinase AKT was detectable by Western blot analysis at 60 kDa (phospho-AKT). After *BMF* knockdown, AKT was found in an activated state in IEC and kept on collagen-coated transwells for 24 h, whereas phospho-AKT levels in dying mock-infected cells were clearly lower (Fig. 5*A*). This indicates that survival pathways can be maintained efficiently when cells are protected from apoptosis because of lack of BMF. Following the studies on fragmentation of the nuclei, we addressed the impact of *BMF* knockdown on the activation of caspases, as execution of the caspase cascade initiates degradation of DNA. To investigate the effect of *BMF* knockdown, caspase 3 activation in response to induction of anoikis in whole crypts of human IEC with and without *BMF* knockdown was determined by Western blot analysis (Fig. 5*B*). Mock-treated IEC showed increased levels of active caspase 3, illustrating ongoing apoptosis.

Next, the lentiviral system was used to knock down *BMF* in whole resections of human colonic mucosa. Again, the incubation with virus-containing medium was started immediately after the surgery. In this experiment, after 6 h of incubation in lentivirus-containing medium, human IEC were isolated and kept for 2 h on a whip-shaker for induction of anoikis. Cleavage of caspase 3 was determined in single cells from the first agitation step (Fig. 5*C*). IEC liberated from the basal lamina showed significantly higher levels of activated caspase 3 after mock infection compared with cells with *BMF* knockdown ($n = 6$, Mann-Whitney rank sum test, $p < 0.05$). This indicates a decreased activation of death signals after *BMF* knockdown.

Cleavage of caspases 6 and 7 was determined in lysates from cells collected after the first agitation step (Fig. 5*D*). Here, IEC were again kept in virus-containing media for 25.5 h. Western blot analysis for inactive procaspase 6 (35 kDa) and procaspase 7 (35 kDa) demonstrated that both proteases were activated more effectively in the mock-infected group. Next, we performed a Western blot analysis for activated caspase 3 in IEC of the first, second, and third agitation steps with and without *BMF* knockdown (Fig. 5*E*). Treatment with RNAi for *BMF* knockdown led to lower amounts of active caspase 3. Taken together, these experiments demonstrate that activation of caspases is delayed by *BMF* knockdown.
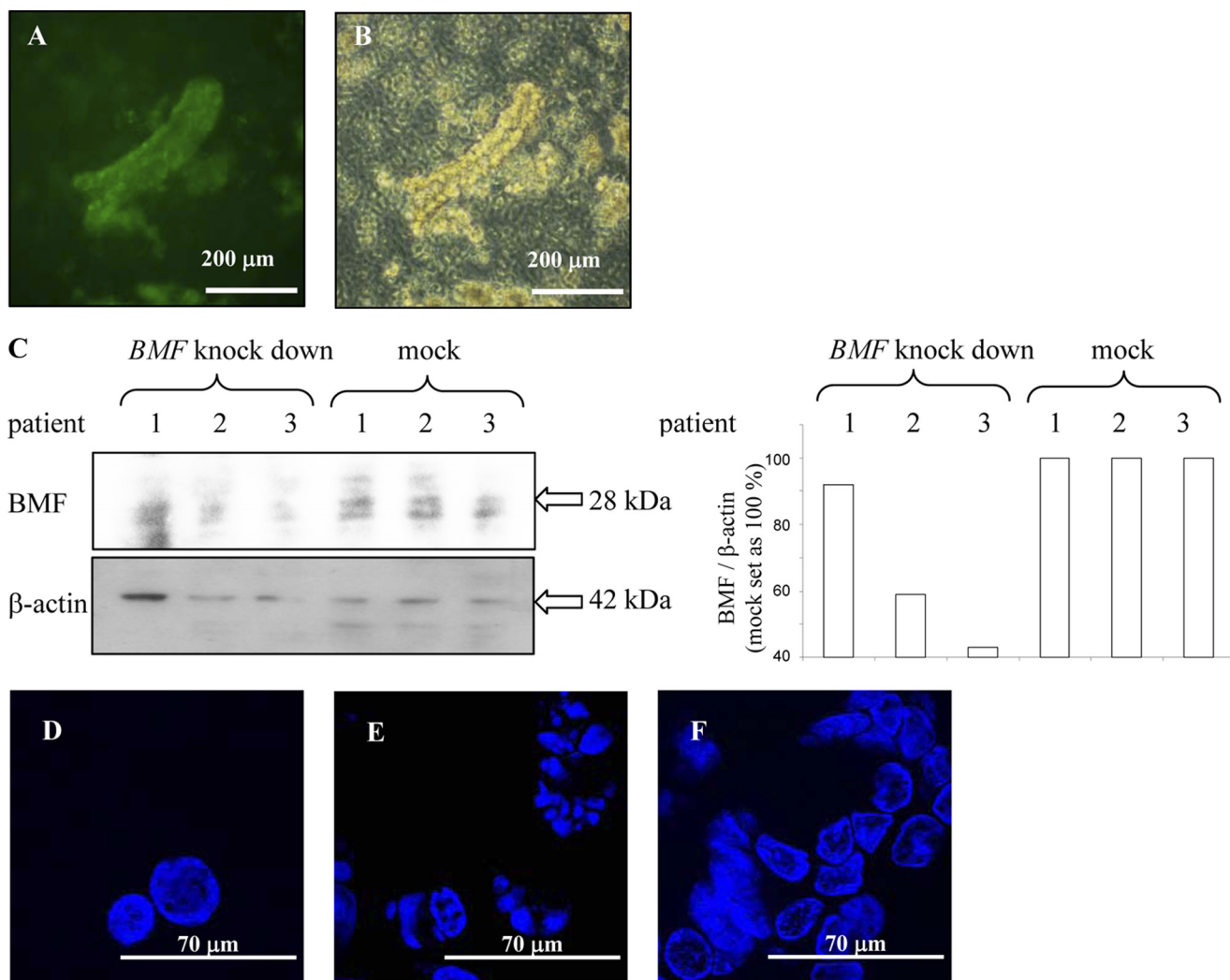
FIGURE 4. **Knockdown of *BMF* in primary human IEC crypts.** Including the transport of the resection from the department of surgery, isolation of crypts, and incubation on transwells, IEC were kept in virus-containing media for 25.5 h. *A*, fluorescent image of crypts infected with lentivirus. *B*, transmission light microscopic image of crypts cultivated on collagen-coated transwells and incubated with trypan blue. *C*, Western blot analysis and densitometry confirms down-regulation of BMF. *D*, fluorescence microscopy of freshly isolated cells. *E*, cells 2 h after induction of anoikis and (*F*) cells with *BMF* knockdown 2 h after induction of anoikis. Knockdown of *BMF* protects against condensation of chromatin. DAPI, × 630. Data are representative for three patients.

DISCUSSION

In this study, we show that down-regulation of BMF suppresses anoikis in primary human IEC *in vitro*. In a second attempt, we used the DSS colitis mouse model to determine BMF dependence of mucosal inflammation. Upon DSS treatment, the weight of $Bmf^{-/-}$ mice was increased significantly compared with wild-type. $Bmf^{-/-}$ mice with and without colitis showed an increased colon length. Crypt lengths for $Bmf^{-/-}$ mice receiving water were increased significantly compared with water-treated wild-type mice. A possible explanation for an increased colon and crypt length could be that the life span of IEC in $Bmf^{-/-}$ mice is longer than in wild-type mice. The proportion of apoptotic IEC compared with the number of total cells in a crypt could be lower in $Bmf^{-/-}$ mice, synonymic with a decreased apoptosis rate of IEC in $Bmf^{-/-}$ mice. A decreased apoptosis rate and unchanged number of dead cells in a crypt at the same time could contribute to the elongation of crypts. This could be protective during onset of inflammation. The histological score for $Bmf^{-/-}$ mice and wild-type mice receiving either water or DSS, however, was not significantly altered at the end of the experiment. Both water-treated groups showed almost no signs of inflammation. Mice from both DSS-treated groups were severely inflamed at the distal end of the colon. Differentiation between both groups was not possible with this parameter.

Human colonic IEC exhibited intense staining in the extrusion zone. Expression of *BMF* in IEC was confirmed by real-time PCR. The technique utilized to isolate IEC requires several successive agitation procedures to discriminate discrete fractions. In consequence of the isolation procedure, both single cells and whole crypts embedded more loosely in the mucosal architecture were supposed to be isolated earlier during the procedure. Adhesion of IEC to the basal lamina was not uniform along the crypt-villus axis. Molecules regulated between crypt and villus, like tenascin and cellular fibronectin, are able to modify cellular adhesion and play a role in IEC shedding (7, 10). Experimental induction of anoikis in human IEC was followed by a significant up-regulation of *BMF*. We showed that
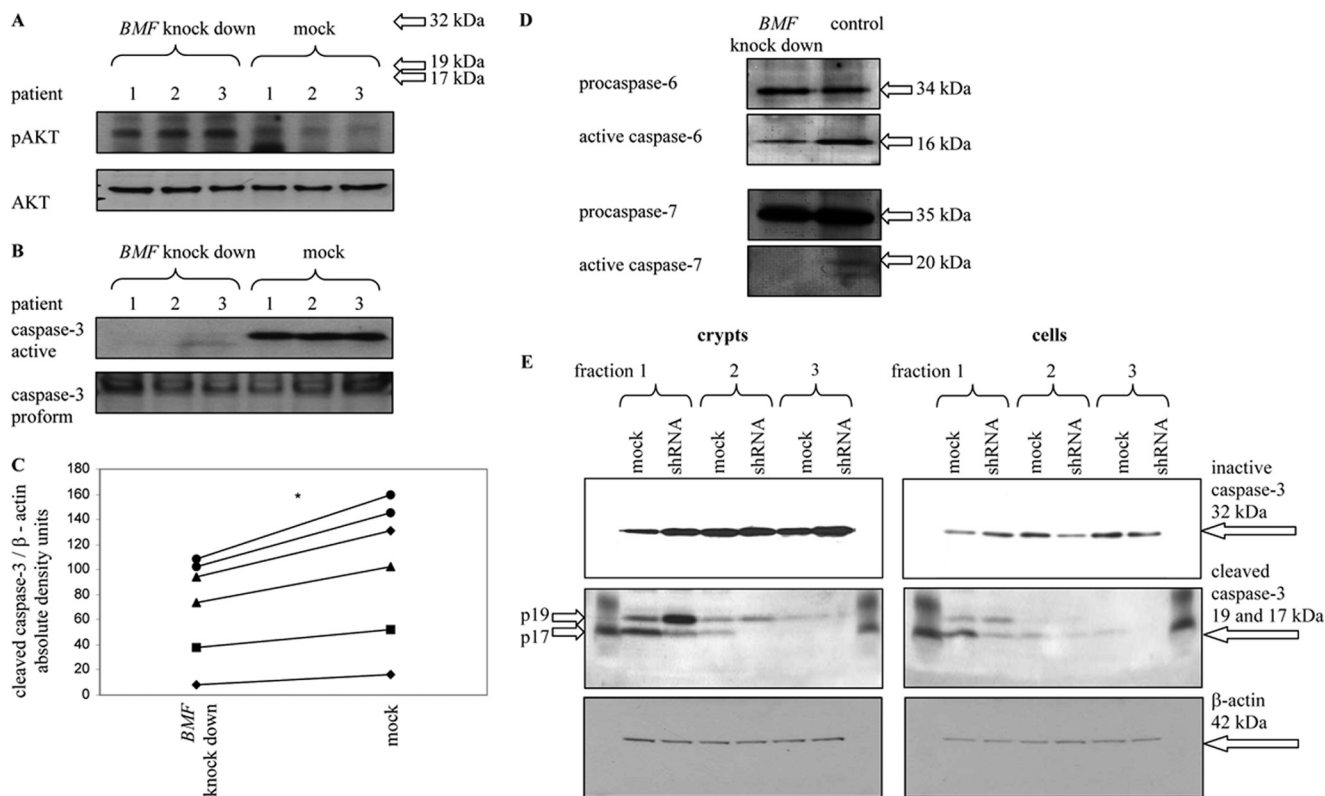
FIGURE 5. **Knockdown of *BMF* maintains the active form of prosurvival factor AKT and the inactive form of caspase 3 in primary human IEC.** *A*, *B*, *D*, and *E*, IEC were kept in virus-containing media for 25.5 h. *A*, phospho-AKT after induction of anoikis in whole crypts with and without *BMF* knockdown. *B*, cleaved caspase 3 after induction of anoikis in whole crypts with (*left lanes*) and without *BMF* knockdown (*right lanes*). Cleaved caspase 3 was normalized to caspase 3 proform. *C*, after 6 h of incubation in lentivirus-containing medium, cleaved caspase 3 after induction of anoikis in single cells with (*left*) and without *BMF* knockdown (*right*). A Mann-Whitney rank sum test was performed. $p < 0.05$, $n = 6$. Patients are not identical to those used in Fig. 5*B*. Cleaved caspase 3 was normalized to β-actin. *D*, knockdown of *BMF* maintains inactivated caspases 6 and 7 in single cells. Data are representative for three patients. *E*, Western blot analysis for activated caspase 3 from IEC of the first, second, and third agitation procedure with and without *BMF* knockdown. IEC from three patients were isolated, and anoikis was induced in both whole crypts (*left panel*) or in a single cell suspension (*right panel*). Western blot analysis for β-actin demonstrated equal loading of the samples. In the isolated, intact crypts, caspase 3 was activated independently of RNAi treatment in crypts from the first and second agitation procedure (4228 and 1853 density units, respectively, in the blot shown). A Mann-Whitney rank sum test was performed. In both cases, treatment with RNAi led to significantly less active caspase 3 (53 ± 21 and 74 ± 39% compared with untreated cells, respectively; $n = 3$, $p < 0.05$). In cells from the third agitation procedure, no activated caspase 3 was detectable. In isolated single IEC, caspase 3 was activated without RNAi treatment in the suspension from all three agitation procedures (3275, 883, and 319 density units, respectively, in the blot shown). *BMF* knockdown led to significantly reduced caspase 3 activity in single IEC from the first and the second agitation procedure (82 ± 57 and 70 ± 30% compared with untreated cells, respectively; $n = 3$, $p < 0.05$). In cells from the third agitation procedure, no activated caspase 3 was detectable. Whole crypts and single cells were isolated by three successive agitation procedures. Data are representative for six patients.

protein levels increase in the mitochondrial fraction upon induction of anoikis in human IEC *in vitro*. This could be due to higher expression levels or translocation. Detachment of IEC, the trigger of anoikis, is associated with *BMF* up-regulation. Cell death is initiated following neutralization of BCL-2 or homologues through association of BMF. We performed knockdown of *BMF* to determine whether cell survival could be prolonged. Knockdown of *BMF* is able to delay anoikis in human IEC, as shown with several assays: Fluorescence microscopy revealed a preserved morphology of the nuclei in knockdown experiments. Activation of the downstream effector caspases 3, 6, and 7 is decreased, as determined by Western blot analysis. The signaling molecule AKT remained in an active state, indicating that the corresponding survival pathways were maintained. Caspase 3 was activated in all single IEC suspensions, but the most prominent effect of *BMF* knockdown was determined in the third agitation fraction. These experiments confirmed differences in successive IEC fractions and indicate that in the latter fraction BMF is decreased, and anoikis is least advanced.

Similar to our experiments, Schmelzle *et al.* (36) investigated the role of BMF in mammary epithelial anoikis. In mammary epithelial cells, anoikis is induced by detachment from the matrix, as in assays performed in the study presented here with colonic IEC. Interestingly, mRNA levels of *BMF* are up-regulated during anoikis upon loss of matrix attachment. Down-regulation of *BMF* expression by RNAi-mediated knockdown is sufficient to prevent anoikis.

BIM, another proapoptotic BH3-only protein family member, also interacts with the prosurvival family member BCL-2. BIM is functionally required for anoikis, and a knockdown of *BIM* also prevents cell death (36). BMF is sequestered to the myosin V motor complex (17) and BIM to microtubule complexes (37), both cytoskeleton-associated structures. Both seem to monitor cytoskeletal integrity. Both proteins counteract the apoptotic activity of prosurvival BCL-2 when vital processes are disturbed. Maturation of IEC along the crypt-villus axis might be defined by different aspects. The spatial arrangement of a cell within a crypt, the genetic programming during maturation (38), the preserva-

tion of cell-cell contacts and cell-matrix anchorage (16), cellular remodeling, or the intracellular damage status of a cell might contribute to the fate of a cell. Inhibition of BMF seems to be a possible medication for epithelial lesions. Others raised the possibility that deletion of BMF would allow survival of tumor cells deprived of matrix interactions outside their natural "niche" (36). BMF was suggested as putative tumor suppressor gene in epithelial solid tumors because it is located on chromosome 15q14 (39), a site frequently lost in metastatic colon cancer, and actively prevents formation of c-myc-driven lymphomas.

In summary, this work describes the sequence of intracellular events during anoikis, a physiological form of apoptosis, in a population of primary human IEC. Our studies narrow down the initiating event leading to the activation of anoikis. Given the stronger expression of prosurvival BCL-2 family members in IEC at the base of the intestinal crypt (40), future studies are underway to delineate the reciprocal expression of its antagonists BMF and BIM.

REFERENCES

1. Gavrieli, Y., Sherman, Y., and Ben-Sasson, S. A. (1992) *J. Cell Biol.* **119,** 493–501
2. Grossmann, J., Walther, K., Artinger, M., Rümmele, P., Woenckhaus, M., and Schölmerich, J. (2002) *Am. J. Gastroenterol.* **97,** 1421–1428
3. Potten, C. S., and Allen, T. D. (1977) *J. Ultrastruct. Res.* **60,** 272–277
4. Sträter, J., Koretz, K., Günthert, A. R., and Möller, P. (1995) *Gut* **37,** 819–825
5. Grossmann, J. (2002) *Apoptosis* **7,** 247–260
6. Frisch, S. M., and Francis, H. (1994) *J. Cell Biol.* **124,** 619–626
7. Beaulieu, J. F. (1992) *J. Cell Sci.* **102,** 427–436
8. Gordon, J. I., and Hermiston, M. L. (1994) *Curr. Opin. Cell Biol.* **6,** 795–803
9. Koretz, K., Schlag, P., Boumsell, L., and Möller, P. (1991) *Am. J. Pathol.* **138,** 741–750
10. Probstmeier, R., Martini, R., and Schachner, M. (1990) *Development* **109,** 313–321
11. Riedl, S., Möller, P., Faissner, A., and Schlag, P. (1992) *EXS* **61,** 277–281
12. Zutter, M. M., and Santoro, S. A. (1990) *Am. J. Pathol.* **137,** 113–120
13. Alnemri, E. S., Livingston, D. J., Nicholson, D. W., Salvesen, G., Thornberry, N. A., Wong, W. W., and Yuan, J. (1996) *Cell* **87,** 171
14. Cohen, G. M. (1997) *Biochem. J.* **326,** 1–16
15. Kemler, R. (1993) *Trends Genet.* **9,** 317–321
16. Hofmann, C., Obermeier, F., Artinger, M., Hausmann, M., Falk, W., Schoelmerich, J., Rogler, G., and Grossmann, J. (2007) *Gastroenterology* **132,** 587–600
17. Puthalakath, H., Villunger, A., O'Reilly, L. A., Beaumont, J. G., Coultas, L., Cheney, R. E., Huang, D. C., and Strasser, A. (2001) *Science* **293,** 1829–1832
18. Grespi, F., Soratroi, C., Krumschnabel, G., Sohm, B., Ploner, C., Geley, S., Hengst, L., Hacker, G., and Villunger, A. (2010) *Cell Death Differ.* **11,** 1672–1683
19. Labi, V., Erlacher, M., Kiessling, S., Manzl, C., Frenzel, A., O'Reilly, L., Strasser, A., and Villunger, A. (2008) *J. Exp. Med.* **205,** 641–655
20. Day, C. L., Puthalakath, H., Skea, G., Strasser, A., Barsukov, I., Lian, L. Y., Huang, D. C., and Hinds, M. G. (2004) *Biochem. J.* **377,** 597–605
21. Kutuk, O., and Letai, A. (2010) *Cell Death Differ.* **17,** 1624–1635
22. Piñon, J. D., Labi, V., Egle, A., and Villunger, A. (2008) *Oncogene* **27,** S41–52
23. Ramjaun, A. R., Tomlinson, S., Eddaoudi, A., and Downward, J. (2007) *Oncogene* **26,** 970–981
24. Suzuki, H. I., Kiyono, K., and Miyazono, K. (2010) *Autophagy*, in press
25. Earnshaw, W. C., Martins, L. M., and Kaufmann, S. H. (1999) *Annu. Rev. Biochem.* **68,** 383–424
26. Salvesen, G. S., and Dixit, V. M. (1997) *Cell* **91,** 443–446
27. Thornberry, N. A. (1998) *Chem. Biol.* **5,** R97–103
28. Grossmann, J., Walther, K., Artinger, M., Kiessling, S., and Scholmerich, J. (2001) *Cell Growth & Differ.* **12,** 147–155
29. Susin, S. A., Zamzami, N., Castedo, M., Daugas, E., Wang, H. G., Geley, S., Fassy, F., Reed, J. C., and Kroemer, G. (1997) *J. Exp. Med.* **186,** 25–37
30. Gumbiner, B. M. (1996) *Cell* **84,** 345–357
31. Pece, S., and Gutkind, J. S. (2000) *J. Biol. Chem.* **275,** 41227–41233
32. Obermeier, F., Kojouharoff, G., Hans, W., Schölmerich, J., Gross, V., and Falk, W. (1999) *Clin. Exp. Immunol.* **116,** 238–245
33. Steidler, L., Hans, W., Schotte, L., Neirynck, S., Obermeier, F., Falk, W., Fiers, W., and Remaut, E. (2000) *Science* **289,** 1352–1355
34. Grossmann, J., Walther, K., Artinger, M., Kiessling, S., Steinkamp, M., Schmautz, W. K., Stadler, F., Bataille, F., Schultz, M., Schölmerich, J., and Rogler, G. (2003) *Eur. J. Cell Biol.* **82,** 262–270
35. Ploner, C., Rainer, J., Niederegger, H., Eduardoff, M., Villunger, A., Geley, S., and Kofler, R. (2008) *Leukemia* **22,** 370–377
36. Schmelzle, T., Mailleux, A. A., Overholtzer, M., Carroll, J. S., Solimini, N. L., Lightcap, E. S., Veiby, O. P., and Brugge, J. S. (2007) *Proc. Natl. Acad. Sci. U.S.A.* **104,** 3787–3792
37. Puthalakath, H., Huang, D. C., O'Reilly, L. A., King, S. M., and Strasser, A. (1999) *Mol. Cell* **3,** 287–296
38. Mariadason, J. M., Nicholas, C., L'Italien, K. E., Zhuang, M., Smartt, H. J., Heerdt, B. G., Yang, W., Corner, G. A., Wilson, A. J., Klampfer, L., Arango, D., and Augenlicht, L. H. (2005) *Gastroenterology* **128,** 1081–1088
39. Wick, W., Petersen, I., Schmutzler, R. K., Wolfarth, B., Lenartz, D., Bierhoff, E., Hümmerich, J., Müller, D. J., Stangl, A. P., Schramm, J., Wiestler, O. D., and von Deimling, A. (1996) *Oncogene* **12,** 973–978
40. Merritt, A. J., Potten, C. S., Watson, A. J., Loh, D. Y., Nakayama, K., Nakayama, K., and Hickman, J. A. (1995) *J. Cell Sci.* **108,** 2261–2271